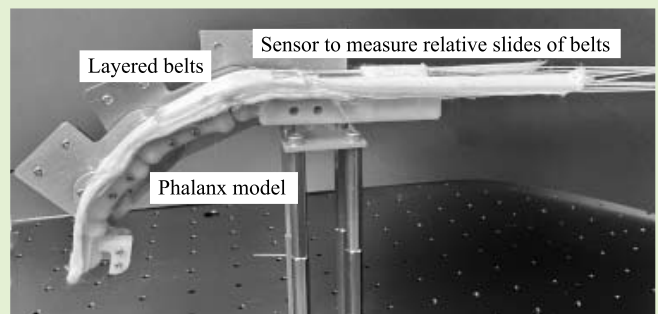


Estimating Finger Joint Motions Based on the Relative Sliding of Layered Belts

Shouhei Shirafuji¹, Member, IEEE, Masafumi Kobayashi, and Jun Ota¹, Member, IEEE

Abstract—This article introduces a new method for measuring finger joints' motion based on the relative sliding motions of belts placed on the finger. Conventional mechanical methods used in wearable devices for measuring hand motions, such as a method using resistive sensors, require calibration for the difference in the fingers' shapes of individuals. In contrast, the proposed method measures the metacarpophalangeal (MP), proximal interphalangeal (PIP), and distal interphalangeal (DIP) joints flex motion of a finger except for the thumb without the above individual calibration using the difference in the sliding amount of belts on the finger surface. The simple equations show that the relative sliding amount of belts is proportional to joint angles with a factor of the belt thickness. Therefore, the method only need to know the belts' thickness beforehand to calculate the joint angles from the relative belt positions but not the fingers' shapes. Experiments with a prototype showed that the proposed method estimated the joint motion of the finger model driven by servomotors with an accuracy of less than 1° in three kinds of motions. The device was in an early stage of development as a data glove, but the accuracies were comparable to other wearable devices. The layered belts mechanism proposed here can provide an option to design a device to realize simplified hand motion measurement by eliminating cumbersome calibration processing for each execution. Furthermore, the simple measurement principle also has an advantage in robustness to noise, such as the drift seen in the devices using inertial measurement units (IMUs).

Index Terms—Belts, goniometers, motion estimation, motion measurement, wearable sensors, wire.



I. INTRODUCTION

HAND manipulation is an essential function for daily life, and the hand is capable of the most subtle motions by the human body. Capturing motions of the hand, especially the fingers, is crucial to understanding hand manipulation, evaluating individual functions for manipulation, and using such information in applications. This has been a motivation to the development of many devices for measuring human finger motions, which include a simple goniometer to a complicated data glove. Recently developed devices for measuring finger motions can be divided into two main types. The first type comprises devices fixed to the environment. The most successful device in this type is the optical motion capture system, which has realized commercial application [1], [2], [3]. This technology has been applied to a wide

range of fields requiring accurate hand motion, such as the teleoperation of robot hands [4] and manipulation in virtual reality (VR) [5]. A significant disadvantage of this type is the complicated setup and requirement of space for cameras. Devices that use changes in an electromagnetic field to measure hand motions have a simpler setup [6] but require wired markers and restrict the environment to no metallic objects around the measurement target. The demand for a compact device with a simple setup has led to the development of hand-tracking techniques that use a single camera [7], [8], depth camera [9], or stereo camera. The leap motion controller system (UltraLeap Ltd., U.K.) is a successfully commercialized device that uses a stereo camera for accurate measurement of hand motions [10], and it has been adopted in many fields, such as gaming in VR and rehabilitation [11] and diagnosis [12] in medicine. However, it has a lower estimation accuracy than motion capture systems [13], and the available space for measurement is limited.

The second type is wearable devices, which include electronic goniometers and data gloves. This type is advantageous, because it avoids spatial requirements or the occlusion of people and objects to cameras. These advantages make this type viable in various situations, such as rehabilitation [14], [15], diagnosis [16], manipulation in VR [17], and teleoperation of a robot [18]. Many researchers have proposed

Manuscript received 3 June 2022; revised 8 August 2022; accepted 11 August 2022. Date of publication 24 August 2022; date of current version 30 September 2022. This work was supported by the JSPS KAKENHI under Grant JP18K13724. The associate editor coordinating the review of this article and approving it for publication was Dr. Cheng-Yao Lo. (Corresponding author: Shouhei Shirafuji.)

Shouhei Shirafuji and Jun Ota are with Research into Artifacts, Center for Engineering, School of Engineering, The University of Tokyo, Tokyo 113-8656, Japan (e-mail: shirafuji@race.t.u-tokyo.ac.jp).

Masafumi Kobayashi is with Department of Precision Engineering, School of Engineering, The University of Tokyo, Tokyo 113-8656, Japan. Digital Object Identifier 10.1109/JSEN.2022.3200017

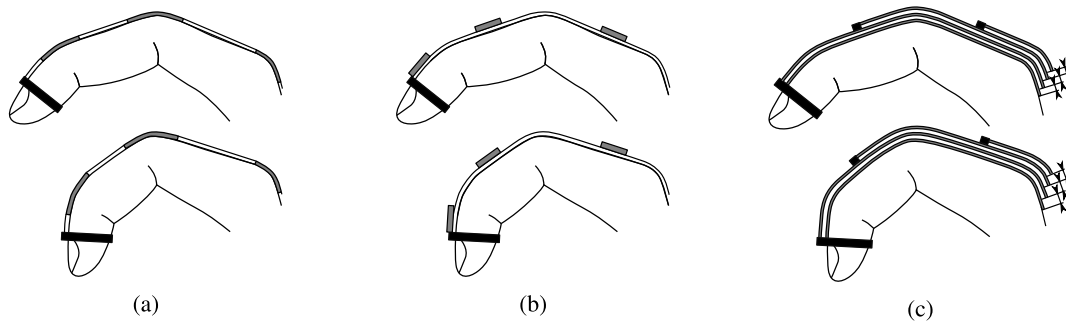


Fig. 1. Different approaches to measuring joint angles. (a) Resistive sensors measure the local deformation of the finger surface. (b) IMUs measure the relative motion between finger phalanges. (c) Our proposed method measures the relative sliding motions of layers with a constant thickness.

measuring finger joint angles using various sensors to realize accurate but compact wearable devices for capturing hand motions. Resistive sensors, such as strain gauges, are the most commonly used for this approach. Wearable devices that use resistive sensors to measure hand motions are effective because of their compactness, reliability, ease of use, and low price. CyberGlove (Cyberglove Systems LLC, USA) is one of the most well-known commercial products that use this approach [19], but many other similar devices have been developed as well [20], [21], [22]. Fiber-optic sensors are also widely used in wearable devices for measuring hand motions, because they offer flexibility and a lightweight [23], [24]. Fig. 1(a) shows how resistive and fiber-optic sensors detect deformation; change in the curvature of the finger surface according to joint flexion causes the change in the resistance and wavelength, respectively. These outputs of sensors depend on the curvature of the finger surface and where they attach to the finger. The curvature differs between individuals, and the sensors' location on the finger slightly changes between the trials. Therefore, these sensors, especially resistive sensors, require calibration for the accurate measurement of joint angles [25], [26], [27]. Alternatively, small inertial measurement units (IMUs) can be placed on each finger phalange to measure the joint angles directly based on the relative motion estimated by the IMUs [14], [28], [29], [30], [31], as shown in Fig. 1(b). While the measurement is not affected by the shapes of the fingers, IMUs are difficult to handle because of their high sensitivity to external and internal noise, which causes drift in the pose estimation [32]. Furthermore, changes in the placement of IMUs also affect their measurement accuracy. This IMU's instability or the cumbersome calibration for the individual finger shapes described above is a barrier to developing wearable applications that can be used easily, such as physical rehabilitation of patients and gaming in VR, allowing the user to start immediately after putting the glove on. Thus, a wearable device for measuring the motions of a human hand is ideally based on a reliable and simple mechanism that does not require calibration to individuals for practical application.

A new method based on our previous work on measuring lumbar spinal motion [33] realizes the estimation of finger joint angles without depending on an individual finger shape. The basic idea of the method and the mechanism to realize

it is the following. The proposed method uses a simple mechanism consisting of layered belts placed along the finger surface, as shown in Fig. 1(c). The shapes of the overlapping regions of the belts are similar to each other in Euclidean geometry, which means their scaling is different, but the shape is the same. Furthermore, the outer curves of these regions are congruent by uniform scaling, and the thicknesses of the belts and the joint angle enable the calculation of the difference in lengths of the curves. This relationship means that the differences in lengths of the outer belt surfaces and their thicknesses give the estimation of the joint angle. The proposed method lets us estimate several joint angles by overlapping an appropriate number of belts and fixing their ends at appropriate points and realizes direct measurement of joint angles with a simple mechanism, and it does not require calibration for individuals.

The main aim of this article is to prove this new method through validation experiments, introducing the proposed method. Section II introduces the relationship between the lengths of overlapped belts and joint angles in more detail. Section III presents the experiment performed to validate the proposed method, where the joint angles of a serial link system were estimated. Section IV concludes this article and discusses future works and potential applications of the proposed method.

II. METHOD

The proposed method is based on our previous work on estimating the rotational center of the lumbar spine and its motion [33]. Here, how the proposed method measures finger motions is introduced. The scope is limited to motions of the finger's metacarpophalangeal (MP), proximal interphalangeal (PIP), and distal interphalangeal (DIP) joints except for the thumb within the sagittal plane (i.e., flexion and extension, not adduction and abduction). However, the proposed method is applicable to 3-D motions in principle. Fig. 2 shows a model of the relationship between the motions of finger phalanges and a belt placed on the finger. Only the distal and medial phalanges are shown for simplicity, and the distal phalange moves around the medial phalange. The followings are the assumptions for simplification.

- 1) The belt thickness is constant during the finger's motion. In reality, the thickness of the belt changes as it bends

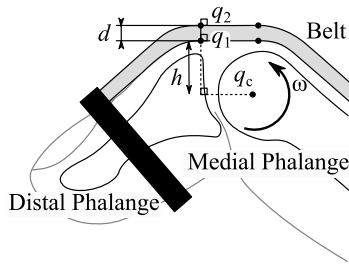


Fig. 2. Model showing the relative motions of phalanges along the sagittal plane and the placement of a belt on the finger surface.

to maintain its volume, although the amount of change depends on the belt material. A mechanism to satisfy this assumption is proposed in Section III.

- 2) The phalanges are rigid bodies. As further assumption, the skin between the phalanges and belt has a constant thickness during finger motion, because the dorsal skin of a finger is normally thin with low elasticity [34].
- 3) The belt is firmly fixed to the fingertip of the distal phalange.

The shape of the belt changes according to the phalange motion. Let the belt thickness be d , and let the lower and upper points where the belt starts bending on the distal phalange be q_1 and q_2 , respectively. The line passing through those points is perpendicular to the belt, because the outer and inner surfaces of the belt share centers of curvature. The belt is straight from those points to the points where the belt starts bending on the medial phalange; this segment is parallel to the common tangent line between the distal and medial phalanges. The location of an instant center of rotation and the angular velocity around it can represent the relative motion between two rigid bodies in a plane. Let the location of an instant center of rotation for relative motion between the distal and medial phalanges be q_c and the angular velocity be ω . Let the distance from the center of rotation to the straight segment of the belt be h . This motion results in the belt sliding along the finger. Two wires placed along the lower and upper surfaces of the belt enable us to measure the difference between the sliding distances of those surfaces, as shown in Fig. 3. The wires are fixed to the end of the distal phalange with the belt. The wires at q_1 and q_2 move by the rotation ω at the velocities v_1 and v_2 , respectively. The angular velocity ω and the velocities v_1 and v_2 have the following relationship:

$$v_1 = r_1 \omega \quad (1)$$

$$v_2 = r_2 \omega \quad (2)$$

where r_1 and r_2 are the distances from the center of rotation to q_1 and q_2 , respectively. The velocities are resolved into parallel and vertical directions with respect to the straight segment of the belt, as shown in Fig. 3. The velocities in the parallel direction of the belt instantaneously slide the wires, and let them be $v_{1\parallel}$ and $v_{2\parallel}$. The geometric relationship between the points on the wires and the center of rotation is given by

$$v_{1\parallel} = v_1 \frac{h}{r_1} \quad (3)$$

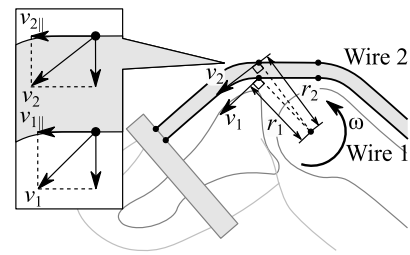


Fig. 3. Model of wires sliding along the lower and upper sides of a belt during the relative motion of phalanges.

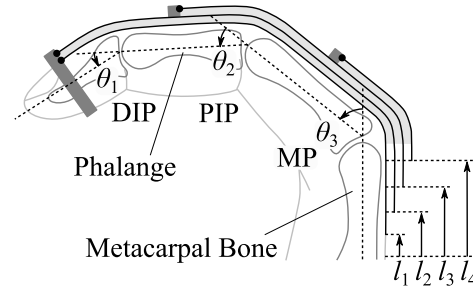


Fig. 4. Model of the relationship between displacements of four wires placed between three belts and the joint angles for three finger phalanges and the metacarpal bone.

$$v_{2\parallel} = v_2 \frac{h+d}{r_2}. \quad (4)$$

Substituting (1) and (2) into (3) and (4) gives

$$\omega = \frac{v_{2\parallel} - v_{1\parallel}}{d}. \quad (5)$$

Equation (5) shows that it is possible to measure the angular velocity by measuring the relative sliding velocity of two wires placed on the lower and upper surfaces of the belt if the belt thickness d is constant. Simple integration of the relative angular velocity of the phalanges and sliding velocities of the wires gives the following relationship between the joint angle and wire displacements if d is constant during finger motions:

$$\theta = \frac{l_2 - l_1}{d} + c \quad (6)$$

where c is a constant of integration, θ is the joint angle between the two phalanges, and l_1 and l_2 are the displacements of the lower and upper wires, respectively. The advantage of this method is that the joint angle between phalanges can be measured directly if the belt thickness is known without requiring any information about individual phalanges.

Equation (6) shows the calculation of a single joint angle from the displacement of wires placed along the lower and upper sides of a belt. This calculation means it is possible to follow the joint angle while the joint moves by measuring the change of wire displacements. The extension of this calculation realizes the estimation of multiple joint angles during a finger motion by overlapping belts on the finger and measuring their relative sliding motions using wires placed on these belts. Fig. 4 shows how the proposed method measures the following finger joints: DIP, PIP, and MP. Let the angles of these joints be θ_1 , θ_2 , and θ_3 , respectively. The mechanism of the proposed method consists of three belts, and the bottommost belt is

fixed to the distal phalange. Let all belts have a constant thickness d during finger motions. Two wires run along the lower and upper surfaces of the belt from the belt ends. The displacements of the lower and upper wires along the metacarpal bone are represented by l_1 and l_2 , respectively. The difference between these displacements is proportional to the sum of the joint angles

$$\theta_1 + \theta_2 + \theta_3 = \frac{l_2 - l_1}{d} + c_1 \quad (7)$$

where c_1 depends on the initial joint angles and wire displacements. The second belt is fixed to the bottom belt on the medial phalange, and a wire runs on it from the fixed point of the belt. The relative sliding motion of this belt only depends on the PIP and MP joints, because this belt and wire follow the bottom belt as it slides up to its fixed point. Let this wire's displacement on the metacarpal bone be l_3 . Then, l_3 has the following relationship with the belt thickness and joint angles:

$$\theta_2 + \theta_3 = \frac{l_3 - l_2}{d} + c_2 \quad (8)$$

where c_2 also depends on the initial joint angles and wire displacements. Finally, the top belt is fixed to the second belt on the proximal phalange, and a wire is also fixed to the same point. In the same manner, let l_4 be the displacement of this wire. This results in the following relationship:

$$\theta_3 = \frac{l_4 - l_3}{d} + c_3 \quad (9)$$

where c_3 is a constant. Herein, c_1 , c_2 , and c_3 are zero if the appropriate joint angles and wire displacements are set. From (7)–(9)

$$\theta_1 = \frac{l_2 - l_1}{d} - \frac{l_3 - l_2}{d} \quad (10)$$

$$\theta_2 = \frac{l_3 - l_2}{d} - \frac{l_4 - l_3}{d} \quad (11)$$

$$\theta_3 = \frac{l_4 - l_3}{d} \quad (12)$$

are obtained. Equations (10)–(12) can be used to estimate the three joint angles of a finger based on the measured displacements of the four wires on the metacarpal bone. The resistive sensor approach often used in data glove is calibrated by measuring the nonlinear relationship between the curvature-dependent resistance of the sensor and these angles for each user in advance. In contrast, (10)–(12) show that the joint angles are proportional to the displacements of the wires with a factor of the belt thickness. If the thickness of the belt is known, it is easily possible to follow the finger's motion by measuring wire displacements. Therefore, it does not require calibration for individuals, because it does not depend on the curve shape of the finger surface, which is different between users. In addition, it is essential to note that (10)–(12) directly relate wire displacements to joint angles, not angular velocities or accelerations. This direct angle measurement makes the measurement more stable than the integration of angular velocity using an IMUs, which is another major approach for data gloves.

Furthermore, the number of sensors to measure the displacements of wires can be reduced by directly measuring

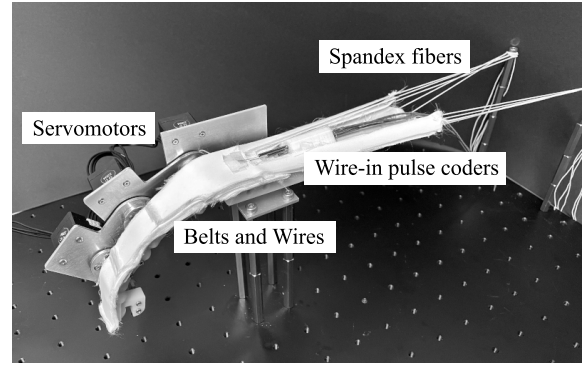


Fig. 5. Experimental system used to validate the proposed method: a serial joint link system with servomotors, belts and wires, and sensors to measure the wire displacements.

the relative displacements of wires on the belts. For example, estimating the joint angles is possible by placing the sensor's base on the bottom of the lowest belt and measuring the other three wires' displacement for this base. Let those relative displacements be

$$l_{12} = l_2 - l_1 \quad (13)$$

$$l_{13} = l_3 - l_1 \quad (14)$$

$$l_{14} = l_4 - l_1. \quad (15)$$

Equations (10)–(12) are rewritten using them as

$$\theta_1 = \frac{2l_{12} - l_{13}}{d} \quad (16)$$

$$\theta_2 = \frac{2l_{13} - l_{12} - l_{14}}{d} \quad (17)$$

$$\theta_3 = \frac{l_{14} - l_{13}}{d}. \quad (18)$$

In the experiment to validate this method in Section III, the above way to estimate joint angles from three wires' displacements is adopted.

III. EXPERIMENT

The validation of the proposed method is conducted using the prototype of the device and the serial joint link system with servomotors instead of a finger for stable verification, as shown in Fig. 5. Specifically, the validation aims to test whether the relative displacements of the three belts enable us to estimate the joint angles during finger motion and their accuracy. The joint angles estimated from measured relative displacements of the belts are compared with the joint angles directly measured by the rotation angle sensors embedded in servomotors. The estimation with the proposed system is applied to two different shapes of links that imitated human finger bone shapes to validate the proposed method is that unaffected by target finger shapes.

A. Experimental Setup

The serial joint link system consisted of three revolute joints corresponding to the PIP, DIP, and MP joints of a finger.

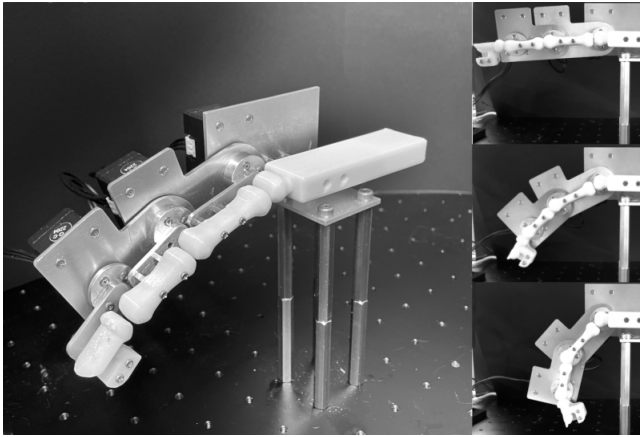


Fig. 6. Serial joint link system consisted of three revolute joints with resin models of a human phalanx and its motion.

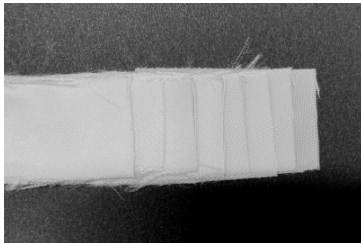


Fig. 7. Belt comprising layers of eight nylon fabrics.

The 3-D printed resin models of a human phalanx are attached to the link system's frames, as shown in Fig. 6. The sizes of the phalange models are approximately the size of an adult middle finger. Servomotors (XL330-M288-T, ROBOTIS Company Ltd., South Korea) are on the joints to drive the links independently. The model of the distal, middle, and proximal phalange moves by the rotation of these motors, respectively. The magnet encoders in the servomotors obtain each joint angle with a resolution of 0.0879° . The joint angles obtained by these encoders while the link system moves were used as the ground truth of the estimation.

In the experiments, the mechanism of the proposed method comprising three belts, three wires, and sensors for wires' displacement is mounted on the phalange models of the joint link system, as shown in Fig. 5. The belts work to keep the wires at a constant distance vertically from the surface of the phalanx regardless of the finger joint angles. Thicker belts between the wires would increase the relative shift between wires, according to (10)–(12) and (16)–(18). Therefore, increasing the belt thickness would increase the angle estimation accuracy based on the sensitivity of the sensors to the wire displacements. However, a thicker belt would have a higher bending elasticity, which would prevent the contact of the belts with the curved surface of the joint. To overcome this tradeoff, layered flexible nylon fabrics were used as a belt, as shown in Fig. 7. Each fabric was 0.25-mm thick and 15.00-mm wide. The fabrics are glued at only one of the ends. The parts of fabrics layered without being sewn or glued together realize a high bending elasticity keeping contact

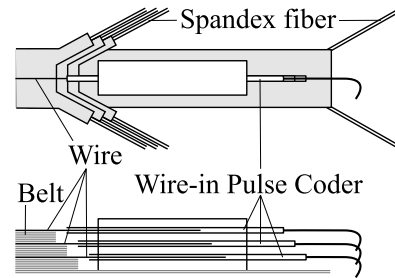


Fig. 8. Structure of system used to measure the wire displacements.

with the finger surface by the fabrics smoothly sliding each other. Fig. 7 shows the structure of a belt composing eight nylon fabrics. The belt had a total thickness of 2.00 mm. The structure of the belt realized a low bending elasticity to fit the curved surface and a constant belt thickness during relative sliding motions. These properties were essential to ensure that the assumptions described in Section II held. As explained in Sections I and II, the proposed mechanism consists of three belts placed on the finger surface. In the experiment, the end of the bottom belt was directly glued to the nail part of the distal phalange model for stability, assuming it would be firmly fixed to a fingertip or nail by a band or glue in actual applications. The ends of the middle and top belts were fixed to the belt underneath in the order explained in Fig. 4. The other sides of the belts were allowed to shift as the belts bent according to joint flexion. Two spandex fibers attached to the top nylon fabric of each belt apply a tensile force to the belt, respectively, as shown in Fig. 8. Additional nylon fabric is placed under the bottom belt to place the sensor to measure relative slides of the belts, and another pair of spandex fibers also pull this fabric. Spandex fibers were adopted here because of their nonlinear elasticity, such as rubber elasticity. A spandex fiber shows the property that the increase in the pulling force becomes moderate according to its extension. This property is helpful to prevent the rise of pulling force on the belts for finger flexion and avoid the problems on the fixation of the belts on the fingertip or the problem in user comfortability. The belts were made based on the size of the middle finger model used in the experiment, but it is possible to use it to measure the motion of another finger except for the thumb if the end of each belt is on each phalange. Three wires were attached to the top of the three belts, respectively. A wire-in pulse coder (WP20-030-1S, LEVEX Corporation, Japan) was used to measure the wire displacements caused by the relative slidings of the belts. This tube-shaped sensor measured the displacement of a magnetic wire in the tube based on the change in the voltage waveform caused by the coil's inductance. The stroke of the wire-pulse coder is 30 mm, and its measurement resolution is 0.015 mm. From (16)–(18), the ideal resolution of the joint angle estimation is 0.0075° . Furthermore, the dynamic response of the wire-pulse coder is 4 kHz. Therefore, the proposed system has the potential to capture the motion at 30° per second of each joint, although the other factors, such as the friction between the belts, may affect it. Independent amplifiers connected to the tube-shaped

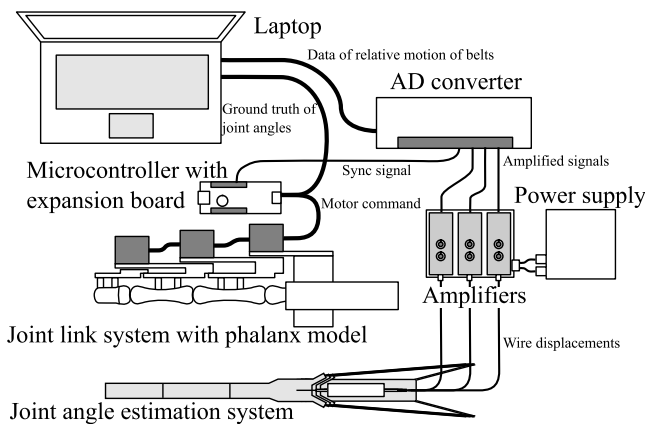


Fig. 9. Schematic of the system used to capture the data obtained by the proposed device for joint angle estimation and joint link system.

sensor by cables amplify the signals. Fig. 9 shows the whole system to control the joint link system and obtain the amplified signals from the wire-in pulse coders. A laptop collected the data through a 16-bit analog-to-digital converter (T7-Pro, LabJack Corporation, USA) at 1 kHz. The data were captured through the official Python application programming interface (API) of the analog-to-digital converter.

The same laptop controlled the joint link system through a microcontroller (Arduino MKR WAN 1310, Arduino, Italy) with an expansion board for the servomotors (DYNAMIXEL Shield for Arduino MKR series, ROBOTIS Company Ltd., South Korea). The control method of the joint link system was a simple proportional control using the PID controller implemented in the servomotors. It was controlled by sending the target position to the servomotors at 10 Hz. As mentioned above, the joint angles were also obtained from the servomotors through the microcontroller at 10 Hz, and its resolution was 0.0879° . For synchronization between the joint angle estimation using the proposed mechanism and the ground truth obtained from servomotors, the analog-to-digital converter recorded the pulse signal from the microcontroller at 10 Hz.

B. Experimental Procedure

The following three procedures compose the experiments conducted to validate the proposed method. First, the wire displacements and joint angles were recorded, while the three joints of the joint link system flexed up to 45° using the wire-in pulse coders and the magnet encoders in servomotors in 10 s. Because of the deformations of components used for routing wires from the belts to the wire-in pulse coders and the properties of the sensors, the wire displacements showed slight nonlinearity for the expected displacements. The above measurement was repeated ten times and compensated for this nonlinearity by obtaining a sextic curve fitting based on measured joint angles. The obtained curve compensates for the wire displacements in the following experiments.

After this compensation, the wire displacements and joint angles were recorded during three kinds of joint motion to evaluate the estimated joint angles from wire displacements by comparing them with the ground truth obtained servomotors. The motions are differences in the target angles of joints to

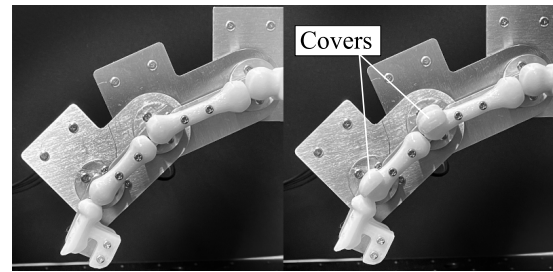


Fig. 10. Covers attached on the ends of phalanx.

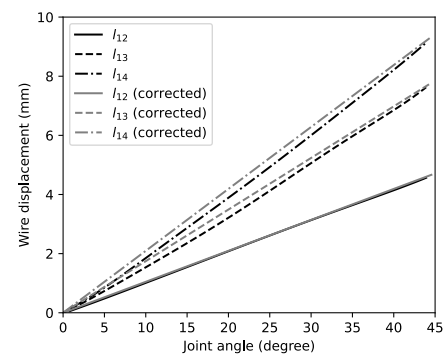


Fig. 11. Change in wire displacements while the three joints flexed up to 45° and corrected displacements based on the ground truth of joint angles.

reach in 10 s; 45° , 30° , and 30° of the MP, PIP, and DIP flexion; 30° , 45° , and 30° of the MP, PIP, and DIP flexion; and 30° , 30° , and 45° of the MP, PIP, and DIP flexion. The start signal from the A–D converter connected to the laptop triggers the motors of the joint link system to move, and the computer starts to record the data from the A–D converter simultaneously. The joint link system moves by setting the appropriate target angles at 10 Hz to reach the target angles in 10 s. After 10 s, the joint link system stops and moves back to the initial posture, where every joint angle is 0° . During the motion, the servomotors send the joint angles used as the ground truth of the estimation to the laptop. They also send the pulse signal simultaneously to the A–D converter to match the ground truth with the estimated angles. The above procedure was repeated ten times for each motion to evaluate the repeatability and stability of the joint angle estimation by checking the estimation variance among trials. The joint angles estimated using (16)–(18) were evaluated by comparing them with the ground truth based on the recorded pulse signal from the microcontroller.

Finally, the system estimated the joint angles for the same three motions with different shapes of the phalanx model. One of the contributions of the proposed method is that the estimation does not require calibration for the difference in the finger shape of individuals, as explained in Sections I and II. This experiment aims to show this insensitivity using the different contact shapes between the belt and the bones with the same measurement condition. The cover was attached to the region of contact between the belt and the bones on the phalanx model, as shown in Fig. 10. The wire displacements and joint angles were recorded during the three joint motions in the previous experiment and compared the estimated joint

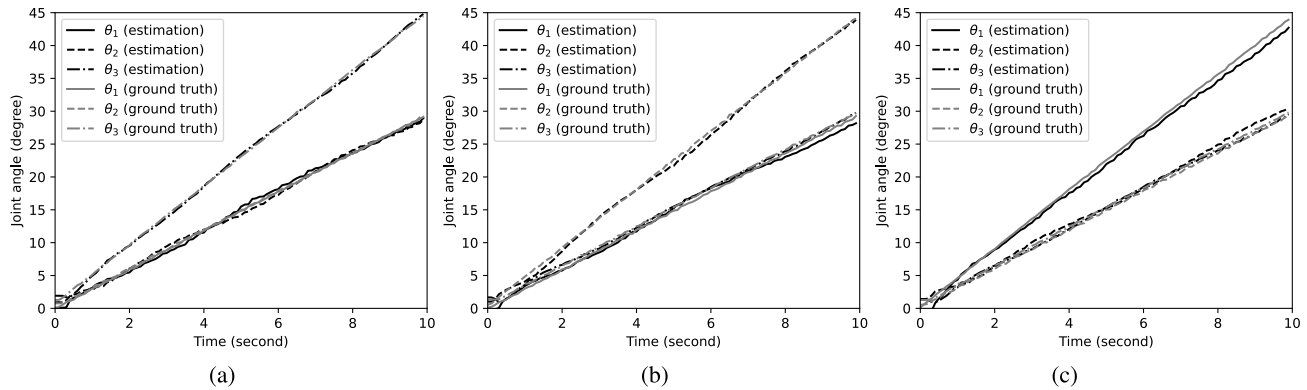


Fig. 12. Mean of estimated joint angles using the proposed method and their ground truth obtained from servomotors while the joints moved in 10 s. (a) 45°, 30°, and 30° of the MP, PIP, and DIP flexion, (b) 30°, 45°, and 30° of the MP, PIP, and DIP flexion. (c) 30°, 30°, and 45° of the MP, PIP, and DIP flexion.

angles with ground truth. The measurement was repeated ten times under each condition.

The estimation of the joint angles was evaluated by comparing with ground truth obtained directly from the servomotors with the root mean square error (RMSE) for the whole ten trials of each motion condition. Furthermore, the stability of the estimation was also evaluated by testing the variance in ten trials, calculating the mean of the standard deviation of the estimated joint angles. These results before and after the change of the phalanx model's bone shapes were compared to evaluate the method's insensitivity to the difference in the finger shape.

C. Results

First, the wire displacements show instability after setting the device on the finger model because of the misalignment of the layered belts and the nylon fabrics composed of the belt. This instability cannot be observed at least after two times of joint flexion of up to 45°. Therefore, the joint flexed two times before the following procedure. The drift was not observed after it at least while the repetition in the following experiments. There is a possibility of wearing out of the fabrics and changing the friction. These tests will be future work to make our proposed mechanism into an application.

Fig. 11 shows the result of the compensation of the nonlinearity of wire displacement measurement based on the initial experiment that the three joints flexed up to 45° in 10 s. Fig. 11 depicts the relationship between the joint angles and the wire displacements. The black lines show the sextic curve obtained by fitting the relationship between the measured joint angles and the wire displacements. From (16)–(18), this relationship must be linear as the gray lines in Fig. 11, but the obtained curves show that the observed relationship has nonlinearity. As mentioned above, the deformations of routing wires from the belts to the wire-in pulse coders and the properties of the sensors possibly cause this nonlinearity. The obtained sextic curve was used to correct the measured wire displacements in the following results.

Fig. 12 shows the estimated joint angles from the corrected wire displacements using the proposed method during three different motions and their ground truth directly

TABLE I
MEAN OF THE RMSEs OF THE ESTIMATED JOINT ANGLES FOR THE MP, PIP, AND DIP JOINTS

Motion	MP joint angle (degree)	PIP joint angle (degree)	DIP joint angle (degree)
1	0.3291	0.4141	0.4269
2	0.2557	0.4655	0.5253
3	0.3353	0.8894	0.8456
1'	0.3195	0.4200	0.7141
2'	0.2757	0.6502	0.4204
3'	0.2733	0.5770	0.9638

TABLE II
MEAN OF THE STANDARD DEVIATION OF THE ESTIMATED JOINT ANGLES OVER TEN TRIALS

Motion	MP joint angle (degree)	PIP joint angle (degree)	DIP joint angle (degree)
1	0.0761	0.0857	0.1316
2	0.0401	0.0786	0.1257
3	0.0394	0.0916	0.1430
1'	0.0556	0.0806	0.2578
2'	0.0377	0.0697	0.0883
3'	0.0479	0.1128	0.1464

obtained from servomotors. The estimated joint angles in Fig. 12 are the mean of ten trials. A slight shift can be seen in the estimated values from their ground truth, especially in the large joint angles. However, the proposed method well estimated the difference in the joint angles during each motion. Table I shows the RMSE of the estimated θ_1 , θ_2 , and θ_3 . Motions 1–3 in Table I correspond to the motions in Fig. 12(a)–(c), respectively. The estimation accuracy was less than 1° in RMSE for all joints and conditions. Table II shows the mean of the standard deviation of the joint estimation over ten trials. The standard deviations were slight among trials concerning the estimation errors. Therefore, the measurement itself is stable, and it seems the errors come from some mechanical problem, such as the nonuniformity of the fabrics. Furthermore, the RMSE and the mean of SD show that the error increases toward the tip of the finger. It seems the frictional force between the fabrics affects this increase of error in the estimation.

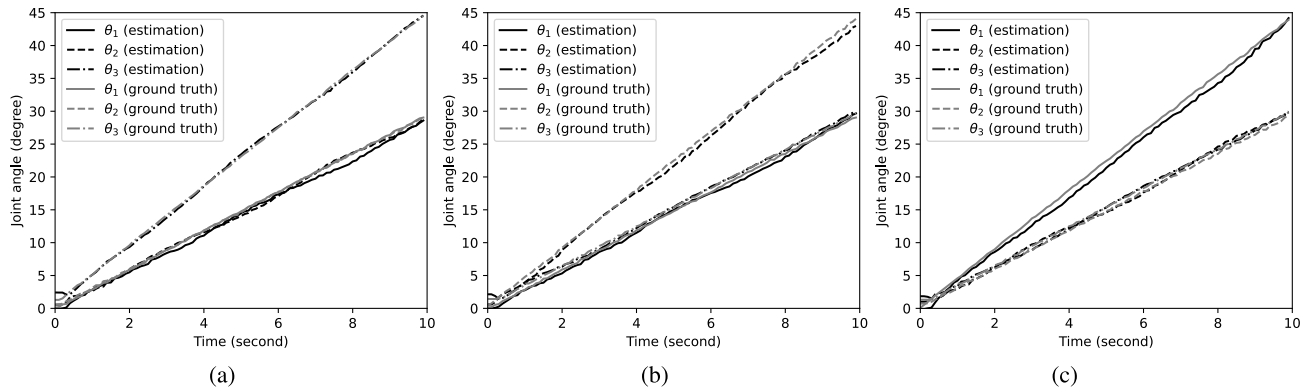


Fig. 13. Mean of estimated joint angles using the proposed method and their ground truth obtained from servomotors while the joints moved in 10 s after the change of the shape of the phalanx model. (a) 45°, 30°, and 30° of the MP, PIP, and DIP flexion. (b) 30°, 45°, and 30° of the MP, PIP, and DIP flexion. (c) 30°, 30°, and 45° of the MP, PIP, and DIP flexion.

Fig. 13 shows the estimated joint angles during three different motions with the same condition of the previous experiment after the change of the shape of the phalanx model by attaching the covers to them. A slight shift can be seen in the estimated values, but the estimated joint angles followed the ground truth in every motion well. Motions 1', 2', and 3' in Table I correspond to the motions in Fig. 13(a)–(c), respectively, and Table I shows the RMSE of the estimation during these motions. The estimation accuracy slightly changed from the previous experiment, but the error is still small, and it was less than 1° in RMSE for all joints and conditions. Table II shows that the mean of the standard deviation was also small after the change of the shapes of the phalanx model. The results show that an accurate estimation is possible even if the shape of the finger is different between the users, and the device does not require calibration for the difference in the finger shape.

IV. CONCLUSION

The proposed estimating method of finger joint angles that does not require calibration to individuals should facilitate the development of a wearable device for easy measurement. The proposed method is just based on measuring the relative sliding motions between belts according to the difference in curvature radii caused by the belt thicknesses. It requires only information about the belt thickness and not about the finger shape of the user. This is a significant advantage, because most of the existing wearable devices for accurately measuring hand motions require calibration to individuals before measurements. Furthermore, the proposed method has a simpler mechanism compared with other methods that do not require calibration for different finger shapes, such as systems using IMUs. It is also an essential advantage that there are no fragile sensors on the finger and only layered fabrics.

The experimental results showed that the proposed method resulted in an RMSE of less than 1°. Although a slight change in accuracy was observed after changing the shape of the finger model, the proposed mechanism kept the accuracy to less than 1°. This is sufficiently accurate compared with other devices that do not depend on the finger shape. For example, Lin *et al.* [30] reported that their device using IMUs

had estimation errors of 1°–2° with a similar experimental setup, although angle estimation errors with IMUs usually become more significant when the hand is moving dynamically [29], [32], because of the integration of unavoidable errors. The mechanism, which directly measures the angles themselves, not velocity or acceleration, has an advantage in stability and reliability. Some commercial devices that require calibration to individual users show high accuracy and stability even in a dynamic situation. For example, CyberGlove guarantees measurement nonlinearity of less than 0.6% over the joint range. Even though the proposed method demonstrated only minor errors in the experiment, the error should be minimized to be competitive with such commercial products. The experimental errors can be attributed to the rigidity of the mechanical components used to guide the belts and wires and the elasticity of the belts. The nonlinearity observed in the wire displacement indicates these problems. Adopting a new belt material that is elastic in bending and that has high tensile strength will help increase the measurement accuracy and stability.

The potential of the proposed method also lies in the fact that its principle of measuring joint angles is very different from other methods. While an optical motion capture system can estimate the joint angles with high accuracy, it usually does not entirely match the actual joint angles, because the markers on the finger slide without careful marker displacement [3], [35]. In contrast, the proposed method directly measures the relative angles between rigid bodies. Theoretically, this means that the sliding motion of the device on the finger should not affect the measurement accuracy. Therefore, the proposed method is a strong option for designing a measurement device for hand motions.

In this study, the validity of the principle of measuring in the proposed method was demonstrated, and the evaluation was conducted only on the model of a human finger. As the device attached to the finger model in Fig. 5, it can be attached to a human hand by fixing the end of the device to the fingertip and fixing the spandex fibers to the wrist. The sliding of the belts on the finger and the sliding of wire-pulse coders on the back of the hand realize the joint angle estimation as the experiments in this article. However, there will be several

problems to apply our joint angle estimation mechanism to practical application from the laboratory environment. First, the belts must be stable on the finger and need to prevent it from slipping off. For example, it is necessary to devise such a way as making it into a glove shape. It is also necessary to consider the influence of the finger's inward and outward motion, which this article ignores. Ideally, these motion does not affect to the estimation of finger motion in sagittal plane, while the belts and wires translate on the MP joint. However, it possibly requires some mechanism to reduce the effect of these motion. There is also the possibility to extend the method proposed here to measure inward and outward motions by routing the belts on this joint axis, but this is one of the future works of this research. Furthermore, the amplifiers of the wire-pulse coders and analog-to-digital converter were placed outside of the device and connected them by cables. From the application viewpoint, they should be implemented inside the device and placed on the hand, but it may be not difficult using specialized circuits for this device. Furthermore, the data were captured through cables in the experiment, but it is better to use wireless communication for a practical application. Finally, the thickness of the belts may cause a problem for practical application. As explained in Section III-C, the belts' thickness coincides the range of wire displacements according to the angle changes. Thinner belts requires a high-resolution sensor to measure relative motion between belts. The high-sensitive and stable displacement sensor is a key to make the proposed mechanism more compact. A most imaginable application of the proposed mechanism is the glove for the VR device. The fabricated glove with a layered-belt structure as shown here will give an accurate hand posture needed to precisely control our hand in VR space for interacting with virtual objects. In this kind of application, the necessity of calibration for compensation of difference of individual hand shape must be a barrier for making it common technology. Further work is needed to realize its practical application considering these problems, but this study showed the possibility of the calibration-free data glove.

ACKNOWLEDGMENT

The authors would like to thank Enago (www.enago.jp) for the English language review.

REFERENCES

- [1] M. Windolf, N. Götzen, and M. Morlock, "Systematic accuracy and precision analysis of video motion capturing systems—Exemplified on the *Vicon-460* system," *J. Biomech.*, vol. 41, no. 12, pp. 2776–2780, Aug. 2008.
- [2] L. Reissner, G. Fischer, R. List, W. R. Taylor, P. Giovanoli, and M. Calcagni, "Minimal detectable difference of the finger and wrist range of motion: Comparison of goniometry and 3D motion analysis," *J. Orthopaedic Surg. Res.*, vol. 14, no. 1, pp. 1–10, Dec. 2019.
- [3] C. Metcalf *et al.*, "Quantifying soft tissue artefacts and imaging variability in motion capture of the fingers," *Ann. Biomed. Eng.*, vol. 48, no. 5, pp. 1551–1556, 2020.
- [4] I. Cerulo, F. Ficuciello, V. Lippiello, and B. Siciliano, "Teleoperation of the SCHUNK S5FH under-actuated anthropomorphic hand using human hand motion tracking," *Robot. Auto. Syst.*, vol. 89, pp. 75–84, Mar. 2017.
- [5] S. Han, B. Liu, R. Wang, Y. Ye, C. D. Twigg, and K. Kin, "Online optical marker-based hand tracking with deep labels," *ACM Trans. Graph.*, vol. 37, no. 4, pp. 1–10, Aug. 2018.
- [6] M. M. Rahman, A. B. M. A. Hossain, M. M. Rana, and K. Mitobe, "Hand motion capture system in piano playing," in *Proc. Int. Conf. Informat., Electron. Vis. (ICIEV)*, May 2013, pp. 1–5.
- [7] C. Zimmermann and T. Brox, "Learning to estimate 3D hand pose from single RGB images," in *Proc. IEEE Int. Conf. Comput. Vis. (ICCV)*, Oct. 2017, pp. 4903–4911.
- [8] A. Spurr, J. Song, S. Park, and O. Hilliges, "Cross-modal deep variational hand pose estimation," in *Proc. IEEE/CVF Conf. Comput. Vis. Pattern Recognit.*, Jun. 2018, pp. 89–98.
- [9] J. Malik *et al.*, "DeepHPS: End-to-end estimation of 3D hand pose and shape by learning from synthetic depth," in *Proc. Int. Conf. 3D Vis. (3DV)*, Sep. 2018, pp. 110–119.
- [10] A. H. Smeragliuolo, N. J. Hill, L. Disla, and D. Putrino, "Validation of the leap motion controller using markered motion capture technology," *J. Biomech.*, vol. 49, no. 9, pp. 1742–1750, Jun. 2016.
- [11] P. Fernández-González *et al.*, "Leap motion controlled video game-based therapy for upper limb rehabilitation in patients with Parkinson's disease: A feasibility study," *J. Neuroeng. Rehabil.*, vol. 16, no. 1, pp. 1–10, Dec. 2019.
- [12] A. H. Butt *et al.*, "Objective and automatic classification of Parkinson disease with leap motion controller," *Biomed. Eng. OnLine*, vol. 17, no. 1, pp. 1–21, Dec. 2018.
- [13] J. Y. Tung, T. Lulic, D. A. Gonzalez, J. Tran, C. R. Dickerson, and E. A. Roy, "Evaluation of a portable markerless finger position capture device: Accuracy of the leap motion controller in healthy adults," *Physiol. Meas.*, vol. 36, no. 5, p. 1025, 2015.
- [14] B.-S. Lin, P.-C. Hsiao, S.-Y. Yang, C.-S. Su, and I.-J. Lee, "Data glove system embedded with inertial measurement units for hand function evaluation in stroke patients," *IEEE Trans. Neural Syst. Rehabil. Eng.*, vol. 25, no. 11, pp. 2204–2213, Nov. 2017.
- [15] L. Dipietro, A. M. Sabatini, and P. Dario, "Evaluation of an instrumented glove for hand-movement acquisition," *J. Rehabil. Res. Develop.*, vol. 40, no. 2, pp. 179–190, 2003.
- [16] J. Connolly, J. Condell, K. Curran, and P. Gardiner, "A new method to determine joint range of movement and stiffness in rheumatoid arthritic patients," in *Proc. Annu. Int. Conf. IEEE Eng. Med. Biol. Soc.*, Aug./Sep. 2012, pp. 6386–6389.
- [17] J. Li, Y. Xu, J. Ni, and Q. Wang, "Glove-based virtual hand grasping for virtual mechanical assembly," *Assem. Autom.*, vol. 36, no. 4, pp. 349–361, Sep. 2016.
- [18] C. L. Fernando, M. Furukawa, K. Minamizawa, and S. Tachi, "Experiencing ones own hand in teleexistence manipulation with a 15 DOF anthropomorphic robot hand and a flexible master glove," in *Proc. 23rd Int. Conf. Artif. Reality Telexistence (ICAT)*, Dec. 2013, pp. 20–27.
- [19] J. H. Buffi, J. L. Sancho Bru, J. J. Crisco, and W. M. Murray, "Evaluation of hand motion capture protocol using static computed tomography images: Application to an instrumented glove," *J. Biomech. Eng.*, vol. 136, no. 12, pp. 1245011–1245016, Dec. 2014.
- [20] P. Weber, E. Rueckert, R. Calandra, J. Peters, and P. Beckerle, "A low-cost sensor glove with vibrotactile feedback and multiple finger joint and hand motion sensing for human–robot interaction," in *Proc. 25th IEEE Int. Symp. Robot Hum. Interact. Commun. (RO-MAN)*, Aug. 2016, pp. 99–104.
- [21] P. T. Wang, C. E. King, A. H. Do, and Z. Nenadic, "A durable, low-cost electrogoniometer for dynamic measurement of joint trajectories," *Med. Eng. Phys.*, vol. 33, no. 5, pp. 546–552, 2011.
- [22] N. Carbonaro, G. D. Mura, F. Lorussi, R. Paradiso, D. De Rossi, and A. Tognetti, "Exploiting wearable goniometer technology for motion sensing gloves," *IEEE J. Biomed. Health Inform.*, vol. 18, no. 6, pp. 1788–1795, Nov. 2014.
- [23] S. Wise *et al.*, "Evaluation of a fiber optic glove for semi-automated goniometric measurements," *J. Rehabil. Res. Develop.*, vol. 27, no. 4, p. 411, 1990.
- [24] E. Fujiwara, M. F. M. Santos, and C. K. Suzuki, "Flexible optical fiber bending transducer for application in glove-based sensors," *IEEE Sensors J.*, vol. 14, no. 10, pp. 3631–3636, Oct. 2014.
- [25] W. B. Griffin, R. P. Findley, M. L. Turner, and M. R. Cutkosky, "Calibration and mapping of a human hand for dexterous telemanipulation," in *Proc. ASME IMECE Symp. Haptic Interfaces Virtual Environ. Teleoperator Syst.* Princeton, NJ, USA: Citeseer, Nov. 2000, pp. 1–8.
- [26] B. Wang and S. Dai, "Dataglove calibration with constructed grasping gesture database," in *Proc. IEEE Int. Conf. Virtual Environ., Hum-Comput. Interfaces Meas. Syst.*, May 2009, pp. 6–11.
- [27] J. Zhou, F. Malric, and S. Shirmohammadi, "A new hand-measurement method to simplify calibration in cyberglove-based virtual rehabilitation," *IEEE Trans. Instrum. Meas.*, vol. 59, no. 10, pp. 2496–2504, Oct. 2010.

- [28] Y. Choi, K. Yoo, S. J. Kang, B. Seo, and S. K. Kim, "Development of a low-cost wearable sensing glove with multiple inertial sensors and a light and fast orientation estimation algorithm," *J. Supercomput.*, vol. 74, no. 8, pp. 3639–3652, 2018.
- [29] K. Kitano, A. Ito, and N. Tsujiuchi, "Hand motion measurement using inertial sensor system and accurate improvement by extended Kalman filter," in *Proc. 41st Annu. Int. Conf. IEEE Eng. Med. Biol. Soc. (EMBC)*, Jul. 2019, pp. 6405–6408.
- [30] B.-S. Lin, I.-J. Lee, P.-Y. Chiang, S.-Y. Huang, and C.-W. Peng, "A modular data glove system for finger and hand motion capture based on inertial sensors," *J. Med. Biol. Eng.*, vol. 39, no. 4, pp. 532–540, Aug. 2019.
- [31] Y. Peng *et al.*, "A flexible dual-modal sensing system for synchronous pressure and inertial monitoring of finger movement," *IEEE Sensors J.*, vol. 21, no. 9, pp. 10483–10490, May 2021.
- [32] B. Guignard *et al.*, "Validity, reliability and accuracy of inertial measurement units (IMUs) to measure angles: Application in swimming," *Sports Biomech.*, vol. 23, pp. 1–33, Jul. 2021.
- [33] Y. Akin, S. Shirafuji, and J. Ota, "Non-invasive estimation method for lumbar spinal motion using flat belts and wires," in *Proc. Int. Conf. Robot. Biomimetics*, Dec. 2017, pp. 171–176.
- [34] Y. Yang *et al.*, "Determination of normal skin elasticity by using real-time shear wave elastography," *J. Ultrasound Med.*, vol. 37, no. 11, pp. 2507–2516, Nov. 2018.
- [35] G. S. Rash, P. P. Belliappa, M. P. Wachowiak, N. N. Somia, and A. Gupta, "A demonstration of the validity of a 3-D video motion analysis method for measuring finger flexion and extension," *J. Biomech.*, vol. 32, no. 12, pp. 1337–1341, 1999.



Shouhei Shirafuji (Member, IEEE) received the Ph.D. degree in information science from Osaka University, Osaka, Japan, in 2014.

He was a JSPS Research Fellow from 2014 to 2015. From 2015 to 2019, he was a Postdoctoral Researcher with The University of Tokyo, Tokyo, Japan, where he has been an Assistant Professor with the Research into Artifacts, Center for Engineering, School of Engineering, since 2019. His research interests include mechanical design, kinematics, robotics, and biomechanics.



Masafumi Kobayashi received the B.S. degree from the Department of Mechanical and Aerospace Engineering, School of Engineering, Tohoku University, Sendai, Japan, in 2017, and the M.S. degree from the Department of Precision Engineering, Graduate School of Engineering, The University of Tokyo, Tokyo, Japan, in 2020.

His research interests include the development of sensor system for the data glove.



Jun Ota (Member, IEEE) received the B.E., M.E., and Ph.D. degrees from the Faculty of Engineering, The University of Tokyo, Tokyo, Japan, in 1987, 1989, and 1994, respectively.

From 1989 to 1991, he was with Nippon Steel Corporation, Tokyo. In 1991, he was a Research Associate with The University of Tokyo, where he became a Lecturer and an Associate Professor in 1994 and 1996, respectively. From 1996 to 1997, he was a Visiting Scholar with Stanford University, Stanford, CA, USA. In 2009, he became a Professor of the Graduate School of Engineering, The University of Tokyo, and a Professor of the Research into Artifacts, Center for Engineering (RACE), The University of Tokyo. Since 2015, he has been a Guest Professor with the South China University of Technology, Guangzhou, China. Since 2019, he has been a Professor of RACE, School of Engineering, The University of Tokyo. His research interests include multiagent robotic systems, embodied-brain systems science, design support for large-scale production/material handling systems, and human behavior analysis and support.

Dr. Ota was a recipient of the Fellowships from the Robotics Society of Japan (RSJ) in 2016 and the Japan Society of Mechanical Engineers (JSME) in 2021.